ACCURACY STUDY OF AIRBORNE LASER SCANNING DATA WITH PHOTOGRAMMETRY

Toni Schenk[1], Suyoung Seo[1], Beáta Csathó[2]

[1]Department of Civil and Environmental Engineering and Geodetic Science
[2]Byrd Polar Research Center
The Ohio State University
Columbus, OH 43210
schenk.2@osu.edu, Seo.1@osu, csatho.1@osu.edu

ABSTRACT

This paper describes an accuracy study of airborne laser scanning data obtained by the Airborne Topographic Mapper (ATM) laser system over Ocean City, Md. The ATM is a conical scanning laser altimeter developed by NASA for precise measurement of surface elevation changes in polar ice sheets, ocean beaches and drainage systems. First, we determine the "internal" accuracy of the system by comparing data from different flight missions. This is followed by a comparison of the merged laser data sets with surface elevations obtained by photogrammetry. Large-scale aerial photographs have been acquired over the test area and an aerial triangulation was performed to determine the exterior orientation parameters. The comparison consists of several experiments that were performed with the digitized photographs and the laser points. First we determine how well the laser points agree with the visible surface as defined by two overlapping images (stereopsis). This is accomplished by backprojecting the laser points to the images based on their exterior orientation parameters. The location of the laser points in the images serve as initial approximations for image matching. We use an adaptive least-squares matching procedure with a variable template size. A non-zero matching vector indicates discrepancies between laser points and photogrammetry. The purpose of the second experiment is to estimate the horizontal accuracy of laser points. One way to accomplish this is to extract linear features and to compare them. Linear features in laser point data sets can only be determined indirectly, e.g. by intersecting planar surface patches. In contrast, linear features in aerial images can be determined directly by an edge operator. We used the Canny operator to extract edges in the images and feature-based matching to find corresponding edges in the stereopair. After describing the procedure, experimental results are reported.

1 Introduction

Laser altimetry is a new technology for rapidly capturing data on physical surfaces. An ever increasing range of applications takes advantage of the high accuracy potential, dense sampling, and the high degree of automation that results in a quick delivery of products derived from the raw laser data. Airborne laser altimetry offers many advantages, including the high precision of the laser points. It appears at the outset that the elevation accuracy is limited by the range accuracy which is assumed to be better than one decimeter. Planimetric errors are often disregarded with the argument that they do not matter on flat surfaces. This view is too simple—the error budget of laser points is far more complex (*Schenk* (2000)). It is important to distinguish between the accuracy potential and the actual results achieved with today's systems.

Several papers report about errors encountered in laser points or surfaces derived from laser points. In The Netherlands, for example, airborne laser altimetry has been extensively used on a nation-wide scale for establishing DEMs and for monitoring coastal erosion. *Huising and Gomes Pereira* (1998) identified elevation errors in overlapping strips on the order of a few decimeters and planimetric errors of more than one meter. Similar elevation errors are also reported in *Crombaghs et al.* (2000).

We present in this paper an accuracy study of airborne laser scanning data obtained by the Airborne Topographic Mapper (ATM) laser system over Ocean City, Md. The ATM is a conical scanning laser altimeter developed by NASA for precise measurement of surface elevation changes in polar ice sheets, ocean beaches and drainage systems. The accuracy of the laser points is estimated by a comparison with elevations and features derived from aerial images by photogrammetric means. Since laser points are not physical tangible it is impossible to carry out an error analysis on a point to point bases. The second section describes a procedure that we call backprojection. Here, laser points are projected back to aerial images that cover the same surface. This backprojection can be thought of as an image formation process—the location of the footprint is imaged just like any other point on the surface. Now we check with a modified least-squares matching approach if the backprojected laser points are in fact conjugate with respect to the gray values that represent the true surface.

The third section is concerned with the planimetric accuracy of laser points. We propose a method whereby linear features are extracted from both sources. This is not directly possible with laser points, however. First, planar surface patches must be found, for example by way of segmentation. This is followed by grouping planar surfaces that most likely belong to the same object. In this case, two neighboring surfaces are intersected resulting in an object boundary. The same boundary can be determined from the aerial images. Here, edges are extracted, matched, and represented in object space. The two edges in object space should be identical in an ideal world. Comparing corresponding edges allows to estimate the planimetric accuracy of laser points.

2 Elevation accuracy obtained by backprojection

2.1 Principle

Fig. 1 illustrates the principle of checking the accuracy of laser points by photogrammetric means. Let $L = \mathbf{l}_1, \mathbf{l}_2, \ldots, \mathbf{l}_n$ be the laser point cloud with $\mathbf{l}_i = [xl_i \ yl_i \ zl_i]^T$ the ith laser point and let s', s'' be an oriented digital stereopair. The location $\mathbf{p}_i$ of laser point $\mathbf{l}_i$ in an image can be determined by the collinearity equation given below in vector notation.

$$\mathbf{p}_i = \lambda \mathbf{R}(\mathbf{l}_i - \mathbf{c}) \qquad (1)$$

with $\mathbf{p}_i = [x_i \ y_i \ -f]^T$ the image coordinates ($f =$ focal length), $\mathbf{R}$ an orthogonal rotation matrix defined by attitude (three angles) of the image, and $\mathbf{c}$ the position of the perspective center. $\mathbf{R}', \mathbf{c}'$ and $\mathbf{R}'', \mathbf{c}''$ are the six exterior orientation parameters of the two images s', s''.
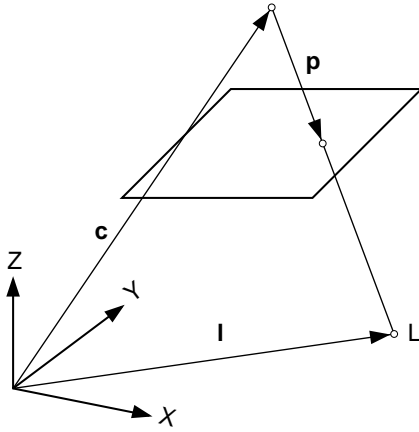

Figure 1: Principle of backprojection. Laser point $\mathbf{l}_i$ is "imaged" in point P_i. The location is found by intersecting line (C, L) with the image plane, mathematically performed by eq. 1.

Images are central projections of the visible surface of the object space. In general, laser points are also on this surface. Hence, when backprojected to the images, one cannot only visualize where the laser footprint was but determine if the computed positions of laser points are really on the surface.

Suppose that laser point L is not on the visible surface as shown in Fig. 2. The computed image positions by eq. 1 are in L' and L'', respectively. At the image location L', surface point A is imaged, however. Likewise, at image location L'', point B is shown. The corresponding point to image point $L' = A'$ is in fact image point A'' and not L''. The difference between L'' and A'' can be determined automatically by area-based image matching (see *Schenk* (1999)).

2.2 Implementation of Backprojection

We have implemented the backprojection method by a modified least-squares matching (LSM) approach. LSM minimizes gray level differences between a template (window in image s' and a matching window of the same size in image s''. The matching window is moved and shaped until the gray level differences reach a minimum. A brief description of the major steps follows.
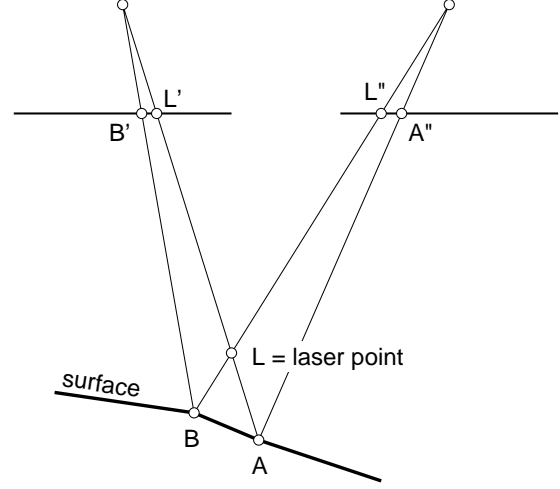

Figure 2: Illustration of the effect of a laser point D that is not on the visible surface. Its backprojected location in the images are in D' and D'', respectively. At these locations, surface points A and B are imaged, however. The corresponding point to $D' = A'$ is A'' and not D''.

1. Backproject laser point $\mathbf{l}_i$ to images s', s'' with eq. 1, using the exterior orientation of the respective images. Convert photocoordinates $\mathbf{p}'_i$ and $\mathbf{p}''_i$ to pixel coordinates row'_i, col'_i and row''_i, col''_i using the affine transformation parameters of the images' interior orientation.

2. Select a template window, centered at row'_i, col'_i that has a distinct gray level distribution. The template size ranges from 9×9 to 23×23 pixels, depending on the gradiants and the entropy. The success of area-based matching depends on distinct gray level variations within the template. If the upper window size is reached without an acceptable entropy, matching is not performed and the method proceeds with the next laser point.

3. Start the iterative LSM approach with the initial position of the matching window centered at row''_i, col''_i. In each iteration, a new position of the matching window is determined. The translation parameters are real values and the gray levels in the new matching window are found by a bi-linear interpolation. The termination criterion is reached if the shift between successive iterations is less than 0.1 pixel.

4. The matched location in s'' is converted to photo-coordinates $(\mathbf{pm}'')$ and intersected with $\mathbf{p}'$—the corresponding point in image s'. This intersected point in object space refers to point A of Fig. 2. The difference between this point and the laser point is used as a quality control measure.

2.3 Experimental Results

A multisensor data set has been collected over Ocean City, Maryland, under the auspices of ISPRS WG III/5, the Geomatics Laboratory for Ice Dynamics of the Byrd Polar Research Center, and the Photogrammetry Laboratory of the Department of Civil and Environmental Engineering, OSU.

The data set comprises aerial photography, laser scanning data, and multispectral and hyperspectral data. *Csathó et al.* (1998) provide a detailed description.

For the experiments we used an aerial stereopair, scanned from the original film negatives with a pixel size of 28 μm. The large scale aerial photographs were flown by the National Geodetic Survey (NGS) at a flying height of 372 m (photo scale approx 1 : 2,435). Thus, the ground pixel size is about 7 cm. We have performed an aerial triangulation of one strip with GPS ground control points. NASA Wallops made several laser data sets available, using the Airborne Topographic Mapper (ATM) laser system. The ATM is a conical scanner, developed by NASA for the purpose of measuring ice sheet surfaces. Recently, other applications have been pursued with this system, for example beach mapping.

The exterior orientation of the photographs is in the same reference frame as the laser points. Consequently, features derived from both data sets can be compared directly.

Fig. 3(a) provides an overview of the test site for the accuracy study. Six areas have been selected. They are highlighted and numbered from 1 to 6. The sub-images are approximately 2×2 cm^2 corresponding to 700×700 pixels. Fig. 3(b) and (c) depict a detail view of area 4. The two sub-images are extracted from the two overlapping digital images that form the stereo model. Superimposed as blue dots are the backprojected laser points. A close visual inspection reveals that the laser points in both images are in fact at corresponding locations. The dense distribution of the laser points results from combining several laser flight missions.

Fig. 3(d) shows the right sub-image. It has been used as the matching image. As described in the previous section, every laser point projected to the left sub-image served as the center of a template while the corresponding point in the right sub-image was used as the starting position of the matching window. In the LSM scheme, the matching window is moved until the gray level differences between template and matching window reach a minimum in the least-squares sense. The red dots in Fig. 3(d) indicate the starting position in the matching window. The end of the red lines depict the final position (matching vector). All the matching vectors are almost horizontal because we applied the epipolar line constraint which forces the match along epipolar lines. Epipolar lines are nearly parallel to the $x-$direction in aerial images. Note that out of 860 backprojected laser points, only 106 could be matched. All the other points did not satisfy the strict criteria imposed on the matching scheme, for example sufficient gray level variation in the template. A good example where this criterion is not met are the laser points on the road. Here, the gray levels within the template and/or matching window are very homogenous and thus not suitable for area-based matching. The same is true for laser points on roofs. Only the building in left upper corner of the sub-image has enough texture to allow matching.

A non-zero matching vector indicates differences between the laser points and the aerial images. We would expect a random error, σ_d of this difference of

$$\sigma_d = (\sigma_a^2 + \sigma_L^2)^{1/2} \qquad (2)$$

with σ_a the standard deviation of an elevation derived from photogrammetry and σ_L the standard deviation of an eleva-

area	#laser points	#matched points	σ_d [m]	bias [m]
1	2870	502	0.12	-0.33
2	2235	461	0.08	-0.42
3	750	217	0.07	-0.02
4	860	106	0.10	0.07
5	1344	207	0.15	-0.33
6	757	108	0.09	0.07

tion error of a laser point. σ_a largely depends on the flying height, the matching method used, and the pixel size. Taking these factors into account we obtain $\sigma_a = \pm 4$ cm. A good estimate for the accuracy of the laser points comes from the comparison and merging of the different laser missions. *Csathó et al.* (2001) provide a detailed report about this comparison from which we assume $\sigma_L = \pm 8$ cm. Hence, the difference should have a standard deviation of $\sigma_d = \pm 9$ cm.

Fig. 3(e) shows the result of the matching procedure. On the horizontal axis are the laser points in ascending order (point number). The blue dots show the difference between laser point elevation and elevation established by matching. The gaps in the horizontal axis indicate points that could not be matched. For an example, see points with a number around 500. The plot reveals a fairly even distribution of the elevation differences around zero. The mean is approximately 7 cm and $\sigma_d = \pm 10$ cm. There are also a couple of outliers clearly visible. For example, point 98 has a $z-$difference of 1.41 m. This point is on the roof of the third building from the top, right upper corner.

In the interest of brevity we omit detailed comments on the other five sub-images. Table 1 summarizes the most important results.

Analyzing Table 1 reveals an average standard deviation of the $z-$differences in all 6 areas of $\sigma_d \approx 11$ cm. This is just about what we have estimated a priori. It confirms the high accuracy of laser points if the systems are well calibrated. The last column of Table 1 contains the bias between laser points and photogrammetry. In some areas, the bias is much larger than the standard deviation. Examining the bias and the corresponding areas suggest that there is a tilt about the $x-$axis of the images (flight direction). Comparing the different laser missions did not indicate a problem of that nature. However, when carefully checking the aerial triangulation results we found that the stereomodel used in this investigation was the last in the strip and it had insufficient elevation control points. Thus, the biases discovered are caused by strip deformation.

Finally, we computed a relative orientation with the total of 1601 matched laser points. The average $y-$parallax was $\pm 2.8\,\mu$m which is exactly $1/10^{\text{th}}$ of the pixel size. This high accuracy does not necessarily reflect the elevation accuracy, however, because errors in the $x-$direction, causing elevation errors, remain undetected.

3 Planimetric accuracy assessment

The planimetric accuracy of laser points has not been thoroughly investigated as judged by the lack of publications dealing with this problem. The primary interest is in elevations and planimetric errors are often neglected with the
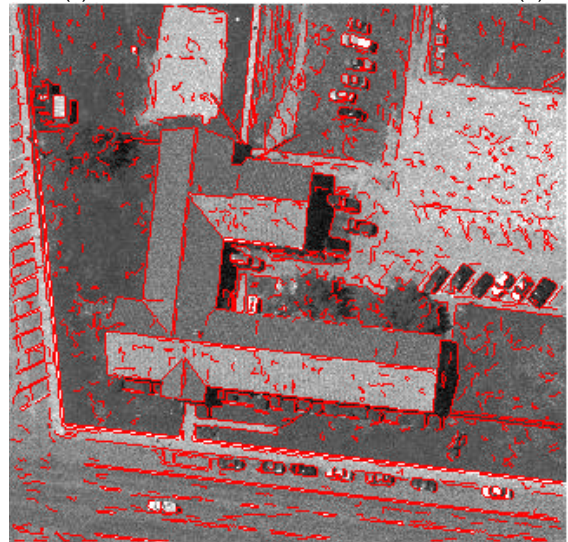
a

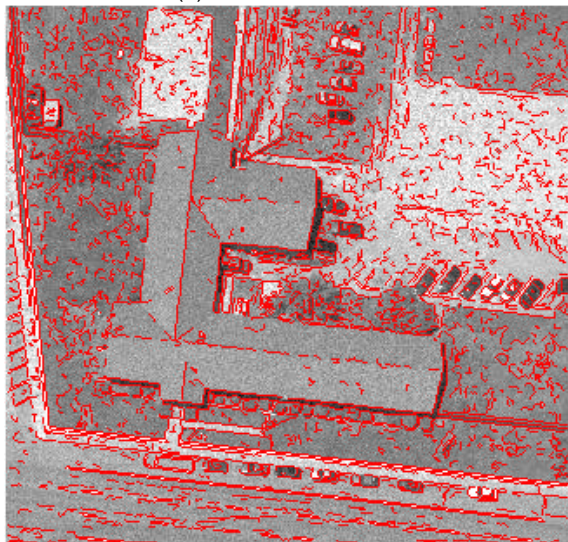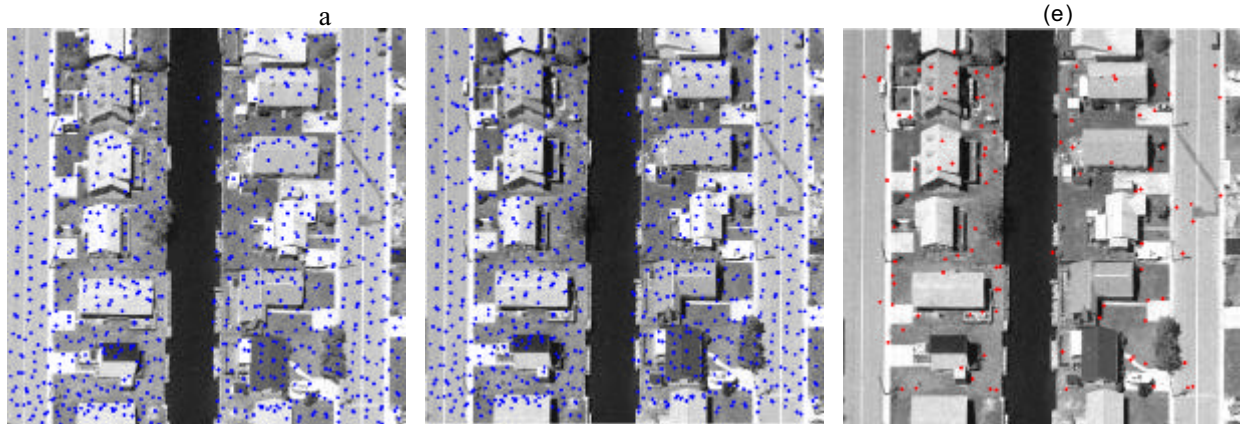N=106 Mean=0.069274 Std=0.24392
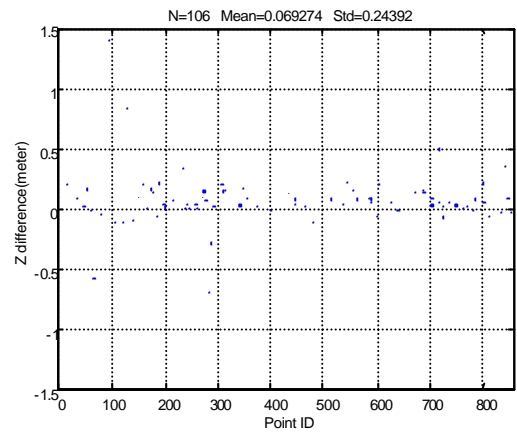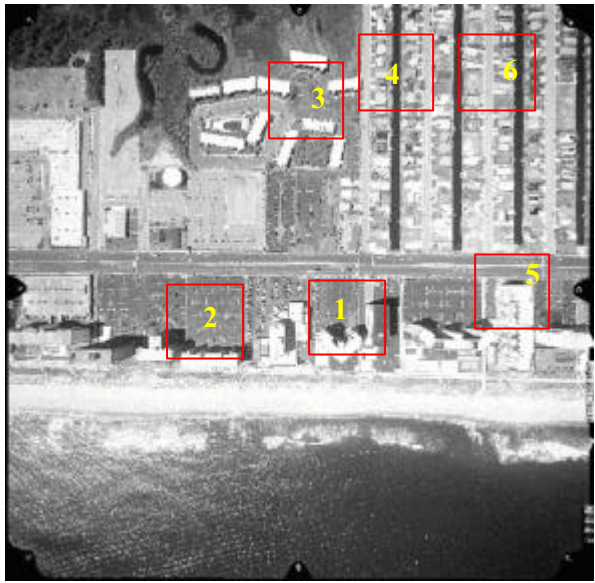
(e)

(b)

(c)

(d)

(f)

(g)

Figure 3: (a) shows the 6 selected sub-areas for checking laser points by the method of backprojection. The backprojected laser points of sub-area 4 are shown in (b) and (c)–a stereopair. The backprojected laser points that passed the criteria for least-squares matching are shown in (d). The z–differences between laser points and matched points in the stereopair are shown in (e). Finally, (f) and (g) shows edges extracted with the Canny operator.

argument that horizontal error components do not cause significant changes in the surface derived from laser points. While this may be true for profiling systems and fairly flat, horizontal surfaces, planimetric errors need attention when scanning systems are used to derive surfaces in rugged topography. Planimetric errors become the primary concern if objects are extracted from a cloud of laser points.

The problem of assessing planimetric errors is rooted in the fact that laser points do not carry semantic information that would allow their physical identification on the ground. By and large, laser points are only defined by location—additional information, such as "top of chimney", "corner of building", "street center line", is missing. Laser footprints are not visible and it will not be possible to directly determine the difference between the footprint (physical location of laser beam on the reflected surface) and the computed laser point.

We describe in this section how to extract physical features from laser points that would allow a comparison with independent determination of the same features.

3.1 Invariant features

Since it is impossible to carry out the accuracy analysis on the level of the original data, one way to solve the problem is to extract invariant features. With this we mean features that are related to object space (visible surface) phenomena. If sensory input data do not contain intrinsic information about the same object space phenomena, tasks such as registration or error analysis cannot be performed. Fortunately, ALS and photogrammetry have implicit information about common features in object space.

We concentrate on linear features, such as object boundaries. Object boundaries are abundant, especially in urban scenes, where man-made objects typically have straight-line or second order curve boundaries. The quest is to determine the same (physical) boundary reliably and automatically from laser points and from aerial images.

Extraction of linear features from laser points There are several ways to determine linear features from a laser point cloud. One possibility, proposed by several researchers, is to interpolate the laser points into a regular grid, and to convert elevations into gray levels (range image), followed by detecting edges in the range image. The rationale is that edges in object space are manifest by abrupt elevation changes. The success of this simple approach hinges on the density of the laser points and the interpolation method used for the conversion of the irregularly distributed points to an image. Unless sophisticated interpolation methods are used that try to avoid interpolating over breaklines, the edges to be detected in the range image are blurred and make it harder to detect them reliably as pointed out, e.g. by *Vosselman* (1999) and *McIntosh et al.* (1999).

Another—in our view better—approach is to compute edges from extracted planar surface patches. This is a lot more robust and leads to edges of superior accuracy as can be shown by simple error propagation. Surface patches (planar or second order surfaces) can be extracted from laser points by way of segmentation. Several segmentation procedures have been proposed (see *Lee and Schenk* (2001) for an overview). A popular approach is to generate a range image for employing segmentation methods developed in image processing. We prefer segmentation methods that

work directly with the irregularly distributed 3D points to avoid potential problems related to the interpolation, however. *Lee and Schenk* (2001) present a multi-stage segmentation scheme with the goal to find a 3D perceptual organization of surface patches.

After having extracted planar surface patches the next problem is to determine which patches should be intersected to generate 3D lines. The challenge is to identify patches that belong to the same object and share a common boundary. Consider a building with a saddle roof, for example. The two planar surface patches extracted from the laser points intersect in the roof line. This is a physical edge, defined by the intersection of two physical planes. Imagine now the intersection of one roof plane with the parking lot next to the building. This intersection also involves two physical planes but it is not physically manifest in the object space. We call this non-physical line a *virtual line (edge)*. Virtual lines may also be useful for establishing planimetric accuracies, however, they are only useful if the same planes can be determined from aerial images.

Apart from topological constraints (adjacent planes in one object), there are also geometric considerations for computing 3D lines. Let us go back to the saddle roof for a moment. The accuracy of the ridge depends on how well the two roofs are determined (e.g. number and distribution of points, fitting plane) and on the intersecting angle, defined by the pitch of the roof. In that regard, virtual edges offer more flexibility in that topological constraints are waived and any two planar surface patches with favorable conditions (their accuracy and intersecting angle) can be chosen.

Extraction of linear features from aerial images Extracting linear features from aerial images is straightforward. There are numerous edge operators available that detect discontinuities in the gray levels, link edge pixels to edges, and assign various attributes, such as strength, orientation, and sign. Figs. 3(f,g) show edges in two overlapping image patches, extracted with the Canny operator. The roof boundaries are successfully detected, but a closer examination reveals that there are gaps in the edges. Also, there are differences between the edges in the left and right image.

The challenge in determining 3D lines from images is in the matching of matching, that is, in the identification of corresponding edges. We employ a feature-based, relational matching scheme and perform the segmentation of matched edges to straight lines in object space, although it is conceivable to determine straight edge segments in image space, before matching.

3.2 Experimental results

We have selected several sub-areas from the same Ocean City data set, described in the previous section. The sub-areas were selected to ensure that planar surface patches could be extracted from the laser point cloud and overlapping aerial images.

Lee and Schenk (2001) describe in detail the procedure of segmenting the laser points into planar surface patches and to group them according to geometric and topologic criteria. The paper also presents results of the segmentation, using the same data set. The planes selected for the experiments described here contained typically more than one hundred points. The fitting error for all planes was less than ± 10 cm,

in many cases as low as ± 5 cm. Thus, a high accuracy for the lines as intersection of two planes can be expected.

The accuracy of lines determined by photogrammetry from aerial images depends on the accuracy of extracted edges in the images, on the exterior orientation parameters, and on the segmentation in object space (fitting a straight line). Taking all these factors into account we can expect the same high accuracy as for lines determined from laser points.

The planimetric accuracy that resulted from comparing eight lines was not consistent. For some lines, the error is slightly higher than expected (about ± 20 cm) while for three lines the error was 40 cm. A closer examination revealed the following interesting problem. The roof ridges computed as intersection of roof planes are not necessarily identical with the physical ridges because they have constructive elements that are not part of the roof planes. This is also apparent in the extracted roof edges. The error of fitting a straight line through the edge pixels in object space also indicates that the physical ridge is not necessarily very straight.

These findings would suggest to avoid a comparison of edges determined by direct measurements of the physical edge (extracting edges in images) with indirectly determined edges (intersection of planes). The dilemma is that physical edges are not directly "mapped" by laser points. On the other hand, determining indirectly edges from images would require point measurements on surfaces, such as roof planes. This, in turn is often times not feasible because many roof planes appear quite homogenous in aerial images (see Fig. 3(f,g) for an example).

4 Conclusions

We have presented an accuracy study of laser points which is based on comparing elevations and features in aerial images with their counterparts in the laser point cloud. The proposed procedure with backprojecting laser points into oriented stereopairs is very successful. The automatic procedure allows to check thousands of points and gives direct information about discrepancies between the laser points and the visible surface as defined by overlapping aerial images. The average elevation difference between 1601 laser points and the photogrammetric surface (stereo) was ± 9 cm. This error consists of errors in photogrammetrically determined points and errors in laser points. Considering the photogrammetric point error we conclude that the laser points have an elevation accuracy of about ± 7 cm.

The method is also suitable for checking the accuracy of DEMs. Here, the grid posts can be backprojected and checked in the same fashion.

Assessment the horizontal accuracy of laser points is an intriguing problem. It can be approached by extracting linear features which are then compared with their "true" location. This is a two step process because linear features can hardly be directly retrieved from laser points. We propose to segment the laser points into planar surface patches and to compute straight lines by intersecting topologically related planes, such as roofs. It is important to realize, however, that these intersecting lines are not necessarily identical with the physical lines. A roof ridge, for example, may be slightly different to the intersection of the roof planes.

We are currently investigating other features that may serve as control information. The prime motivation is to find useful features for fusing aerial images, as well as multispectral and hyperspectral images with laser points obtained from airborne laser scanning systems.

REFERENCES

Crombaghs, M.J.E., R. Brügelmann, and E.J. de Min, (2000). On the adjustment of overlapping strips of laser-altimeter height data. *ISPRS Journal of Photogrammetry & Remote Sensing*, **54**(2-3),164–198.

Csathó, B., Y.R. Lee, T. Schenk, W. Krabill and J. McGarry (2001). Creation of high-resolution, precise digital elevation models of Ocean City and Assateague Island, Md. In *International Archives of Photogrammetry and Remote Sensing*, **34**(3/W4), this proceedings.

Csathó, B., W. Krabill, J. Lucas and T. Schenk (1998). A multisensor data set of an urban and coastal scene. In *International Archives of Photogrammetry and Remote Sensing*, **32**(3/2), 588–592.

Huising, E.J. and L.M. Gomes Pereira, (1998). Errors and accuracy estimates of laser data acquired by various laser scanning systems for topographic applications. *ISPRS Journal of Photogrammetry & Remote Sensing*, **53**(1998),245–261.

Lee, I. and T. Schenk (2001). 3D Perceptual Organization of Laser Altimetry Data. In *International Archives of Photogrammetry and Remote Sensing*, **34**(3/W4), this proceedings.

McIntosh, K., A. Krupnik and T. Schenk, (1999). Utilizing airborne laser altimetry for the improvement of automatically generated DEMs over urban areas. In *International Archives of Photogrammetry and Remote Sensing*, **32**(3/W14), 89–94.

Schenk, T. (2000). *Modeling and Analyzing Systematic Errors in Airborne Laser Scanners.* Technical Report Photogrammetry No. 19, Department of Civil and Environmental Engineering and Geodetic Science, OSU, 39 pages.

Schenk, T. (1999). *Determining transformation parameters between surfaces without identical points.* Technical Report Photogrammetry No. 15, Department of Civil and Environmental Engineering and Geodetic Science, OSU, 22 pages.

Schenk, T. (1999). *Digital Photogrammetry.* TerraScience, Laurelville, Ohio, 428 p.

Vosselman, G. (1999). Building reconstruction using planar faces in very high density height data. In *International Archives of Photogrammetry and Remote Sensing*, **32**(3-2/W4), 383–388.